crystals

MDPI

Article

Co (II) Complexes Based on the *Bis*-Pyrazol-*S*-Triazine Pincer Ligand: Synthesis, X-ray Structure Studies, and Cytotoxic Evaluation

Heba M. Refaat [1,*], Atallh A. M. Alotaibi [1], Necmi Dege [2], Ayman El-Faham [1,*] and Saied M. Soliman [1,*]

[1] Department of Chemistry, Faculty of Science, Alexandria University, P.O. Box 426, Ibrahimia, Alexandria 21321, Egypt; atallh1415@gmail.com
[2] Department of Physics, Faculty of Arts and Sciences, Ondokuz Mayıs University, Samsun 55139, Turkey; necmid@omu.edu.tr
* Correspondence: hebarefaat212@yahoo.com (H.M.R.); aymanel_faham@hotmail.com (A.E.-F.); saied1soliman@yahoo.com (S.M.S.)

Abstract: Four pincer-type Co (II) complexes of the 2,4-*bis* (3,5-dimethyl-1*H*-pyrazol-1-yl)-6-methoxy-1,3,5-triazine ligand (**L**) were evaluated for their cytotoxic activities against lung and breast cancer cell lines using cell viability assay. The X-ray single crystal structure of $[Co(L)(H_2O)_2Br]Br$ (**1**) confirmed the pincer coordination behavior of the ligand **L** as an *N*-tridentate chelate. The hexa-coordination environment of Co (II) is completed by one bromide ion completing the equatorial plane of the octahedral structure and two *trans* water molecules at the axial positions. It crystallized in the monoclinic crystal system and $P2_1/m$ space group with crystal parameters of a = 11.3170(10) Å, b = 7.4613(7) Å, c = 12.6917(12) Å and β = 95.927(3)°. Based on Hirshfeld analysis, the most dominant contacts are H…H (48.8%), Br…H (17.6%), H…C (11.2%) and O…H (10.1%), where the Br…H interactions are the most significant. The cytotoxic evaluation of the studied systems indicated that complex $[Co(L)(NO_3)_2]$ (**4**) has the highest activity against lung (A-549) and breast (MCF-7) cell lines. In contrast, complex $[Co(L)(H_2O)_3](ClO_4)_2.H_2O$(**3**) has the lowest cytotoxic activity against both cell lines.

Keywords: cobalt (II); pincer; *bis*-pyrazol-*s*-triazine; Hirshfeld; cytotoxicity; breast and lung carcinoma

Citation: Refaat, H.M.; Alotaibi, A.A.M.; Dege, N.; El-Faham, A.; Soliman, S.M. Co (II) Complexes Based on the *Bis*-Pyrazol-*S*-Triazine Pincer Ligand: Synthesis, X-ray Structure Studies, and Cytotoxic Evaluation. *Crystals* **2022**, *12*, 741. https://doi.org/10.3390/cryst12050741

Academic Editor: Waldemar Maniukiewicz

Received: 1 May 2022
Accepted: 16 May 2022
Published: 20 May 2022

1. Introduction

s-Triazine and its derivatives are key heterocyclic compounds due to their remarkable chemical behavior and high biological activities. These compounds are associated with interesting pharmaceutical applications, due to their antimicrobial [1–5], anticancer [6–9] and antiviral activities [10]. For example, *s*-triazine aminobenzoic acid derivatives were found to exhibit promising antimicrobial activity [11]. They also showed useful assets in many other applications, such as the fabric, plastic, and rubber industries, and also as pesticides, dyestuffs, optical decolorizes, and explosives [12].

The coordinating capability of multidentate *s*-triazine ligands through nitrogen donor atoms allows the formation of supramolecular associations which possess valuable photosensitive and electrical properties [13]. On the other hand, the concern with metal-based therapy has received increasing attention with respect to efficient schemes in the design of repository, slow-release, or long-acting drugs [14]. In this regard, many organometallic complexes of triazine with different transition metals exerting numerous and sole biological, chemical, and physical properties have been synthesized [15,16]. It is well known that many transition metal complexes have promising biological properties [17–22].

2,4-*Bis*(3,5-dimethyl-1*H*-pyrazol-1-yl)-6-methoxy-1,3,5-triazine (**L**, Figure 1), is a powerful *N*-pincer chelator [23–27] which is used to synthesize many discrete and polymeric metal (II) complexes via a self-assembly technique. Cobalt (II) complexes have well-known

antimicrobial and anticancer activities [28–31], especially those containing *N*-donor ligands. Recently, we reported the synthesis and antimicrobial evaluation of some Co (II) complexes with the *bis*-pyrazolyl-*s*-triazine ligand (**L**) [32]. In continuation to this study, a new Co (II) complex with the same ligand was synthesized and its structural aspects were analyzed using single-crystal X-ray diffraction and Hirshfeld analysis. The main goal of this study is to shed light on the possible biological applications of these Co (II) complexes as anticancer agents.

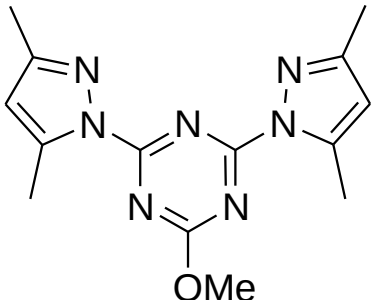

Figure 1. Structure of the ligand (**L**).

2. Materials and Methods

Chemicals and instrumentation, as well as the single-crystal X-ray structure measurement details [33–37], are presented in the Supplementary Materials. Synthesis and NMR characterizations of **L** are described in Figure S1 (Supplementary Materials).

2.1. Synthesis of Co (II) Complexes

Synthesis of the $[Co(L)(H_2O)_2Br]$ Br complex (**1**) was performed by mixing 10 mL methanolic solution of **L** (~0.299 g, 1 mmol) with $Co(NO_3)_2.6H_2O$ (0.291 g, 1 mmol) in 5 mL methanol followed by the addition of 1 mL of saturated KBr aqueous solution. After five days, pink block crystals of **1** were obtained.

Yield: $C_{14}H_{21}Br_2CoN_7O_3$ (**1**) 73%. Anal. Calc. C, 30.35; H, 3.82; N, 17.69; Br, 28.84; Co, 10.64%. Found: C, 30.13; H, 3.73; N, 17.55; Br, 28.68; Co, 10.49. FTIR (KBr, cm^{-1}): 3385 (υ_{O-H}), 3209 (υ_{O-H}), 3079 (υ_{C-H}), 1620($\upsilon_{C=N}$), 1573(Sh; $\upsilon_{C=N}$), 1545($\upsilon_{C=C}$), (Figure S2, Supplementary data).

Syntheses of $[Co(L)(H_2O)_2Cl]Cl$; (**2**), $[Co(L)(H_2O)_3](ClO_4)_2.H_2O$, (**3**) and $[Co(L)(NO_3)_2]$; (**4**) complexes were performed using a self-assembly technique, as reported in our previous study [32].

2.2. Cytotoxic Activity Determination

The cytotoxic activity of **L** and complexes **1**–**4** against lung (A-549) and breast (MCF-7) cancer cell lines was determined. The details of the cytotoxicity determinations are described in Method S1 (Supplementary data).

3. Results and Discussion

3.1. Structure Description of $[Co(L)(H_2O)_2Br]Br$ Complex; (1)

The pincer structure of complex **1** was confirmed by determining its single-crystal X-ray structure (Figure 2). The crystal parameters are a = 11.3170(10) Å, b = 7.4613(7) Å, c = 12.6917(12) Å and β = 95.927(3)° (Table 1). Hence, the complex had crystallized in the monoclinic crystal system. The unit cell volume was 1065.95(17) $Å^3$ and there were two compounds of the formula $[Co(L)(H_2O)_2Br]Br$ per unit cell. The complex crystallized in the centrosymmetric $P2_1/m$ space group with a mirror plane passing horizontally through the skeleton of the organic ligand, Br^- and Co (II) ion. Hence, the asymmetric formula of this complex is half one $[Co(L)(H_2O)_2Br]Br$ unit.

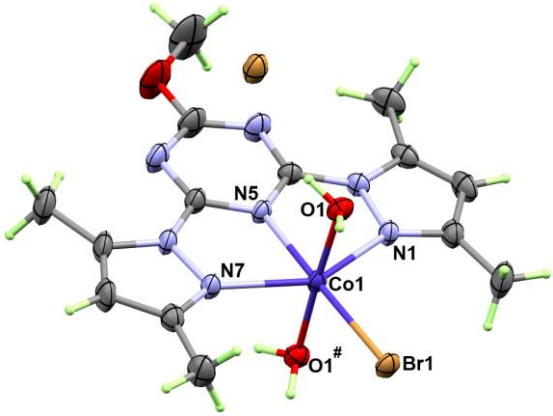

Figure 2. X-ray structure of **1**. Symmetry code for O1$^{\#}$ is x, 1.5 − y, z.

Table 1. Crystal data and refinement details of **1**.

CCDC	**2154990**	
Empirical formula	$C_{14}H_{21}Br_2CoN_7O_3$	
Formula weight	554.13 g/mol	
Temperature	293(2) K	
Wavelength	0.71073 Å	
Crystal system	Monoclinic	
Space group	$P2_1/m$	
Unit cell dimensions	a = 11.3170(10) Å	α = 90°
	b = 7.4613(7) Å	β = 95.927(3)°
	c = 12.6917(12) Å	γ = 90°
Volume	1065.95(17) Å^3	
Z	2	
Density (calculated)	1.726 g/cm^3	
Absorption coefficient	4.582 mm^{-1}	
F(000)	550	
Theta range for data collection	3.17 to 28.33°	
Index ranges	$-15 \leq h \leq 15$, $-9 \leq k \leq 9$, $-16 \leq l \leq 16$	
Reflections collected	24,040	
Independent reflections	2843 [R(int) = 0.0445]	
Completeness to theta = 28.33°	99.60%	
Refinement method	Full-matrix least-squares on F^2	
Data/restraints/parameters	2843/0/161	
Goodness-of-fit on F^2	1.024	
Final R indices [I > 2sigma(I)]	R1 = 0.0440, wR2 = 0.1168	
R indices (all data)	R1 = 0.0687, wR2 = 0.1305	
Largest diff. peak and hole	0.572 and −1.102	

The X-ray structure revealed the pincer coordination behavior of the *s*-triazine ligand (**L**). It acts as a tridentate *N*-chelate coordinated to the Co (II) ion via three Co–N bonds with two nitrogen atoms from the pyrazolyl moieties and one nitrogen from the *s*-triazine core. The corresponding Co–N distances are 2.211(5), 2.226(4), and 2.059(4) Å for Co1–N1, Co1–N7, and Co1–N5 bonds, respectively. As a general trend in similar *s*-triazine complexes [32], the Co–N (triazine) is shorter than the Co–N (pyrazole) bonds (Table 2). The bite angles of the *N*-chelate are 73.62(17) and 73.11(17) for N5–Co1–N1 and N5–Co1–N7, respectively, whereas the N1–Co1–N7 bond angle is 146.73(16). The coordination sphere of Co (II) is completed by two interactions with two symmetrically related water molecules at the axial positions and an interaction with one bromide ion in the equatorial plane, which is located at a *trans* position to the Co–N (triazine) bond. The Co1-O1 and Co1-Br1 bond distances are 2.063(3) and 2.5261(8) Å, respectively. The structure of this cationic complex is completed by another bromide anion (Br2) in the outer sphere. Hence, the coordination geometry of the Co (II) could be described as a distorted octahedral. In the structurally

related $[Co(L)(H_2O)_2Cl]Cl$, the Co–N distances are slightly longer than the corresponding values found in the bromide complex (Table 2). In both structures, the Co–O bond distances are comparable, and of course, the Co–Cl bond in the previously reported structure is shorter than the corresponding value found in the $[Co(L)(H_2O)_2Br]Br$ complex.

Table 2. Selected bond distances and angles for **1** and **2**.

Bond	Distance	Distance [a]	Bond	Distance	Distance [a]
Br1–Co1	2.5261(8)	2.388(9)	Co1–O1$^{\#}$	2.063(3)	2.068(2)
Co1–N5	2.059(4)	2.095(3)	Co1–N1	2.211(5)	2.218(3)
Co1–O1	2.063(3)	2.068(2)	Co1–N7	2.226(4)	2.238(3)
Bond	**Angle**	**Angle**	**Bond**	**Angle**	**Angle**
N5–Co1–O1	91.42(7)	91.18(6)	N1–Co1–N7	146.73(16)	146.38(11)
N5–Co1–O1$^{\#}$	91.42(7)	91.18(6)	N5–Co1–Br1	178.34(13)	178.30(8)
O1–Co1–O1	177.14(15)	177.62(11)	O1–Co1–Br1	88.58(7)	88.82(6)
N5–Co1–N1	73.62(17)	73.01(10)	N1–Co1–Br1	104.72(12)	108.69(8)
O1–Co1–N1	90.22(8)	90.21(6)	N7–Co1–Br1	108.55(12)	104.93(8)
N5–Co1–N7	73.11(17)	73.37(10)			
O1–Co1–N7	90.59(8)	90.47(6)			

[a] The corresponding values for the chloro complex (**2**).

The supramolecular structure of $[Co(L)(H_2O)_2Br]Br$ is controlled by strong O–H…Br hydrogen bonds and weak C–H…Br interactions (Figure 3). A list of the hydrogen bond parameters is presented in Table 3. The perfectly planar ligand backbone is arranged in a highly symmetric fashion in a way which connects the polar regions comprising the coordinated water molecules and bromide anions with the complex units along the crystallographic *b*-direction via strong O1–H1A...Br2 and O1–H1B...Br1 hydrogen bonds in addition to the weak C3–H3A...Br2 interaction. On the other hand, the other two C9–H9A...Br2 and C12–H12...Br2 interactions connected the less polar part (organic ligand) of the complex along the *a*-direction. For simplicity, these weak interactions were omitted from the packing scheme; hence, the supramolecular structure of this complex could be described as 1D hydrogen bonding polymer extended through the *b*-direction.

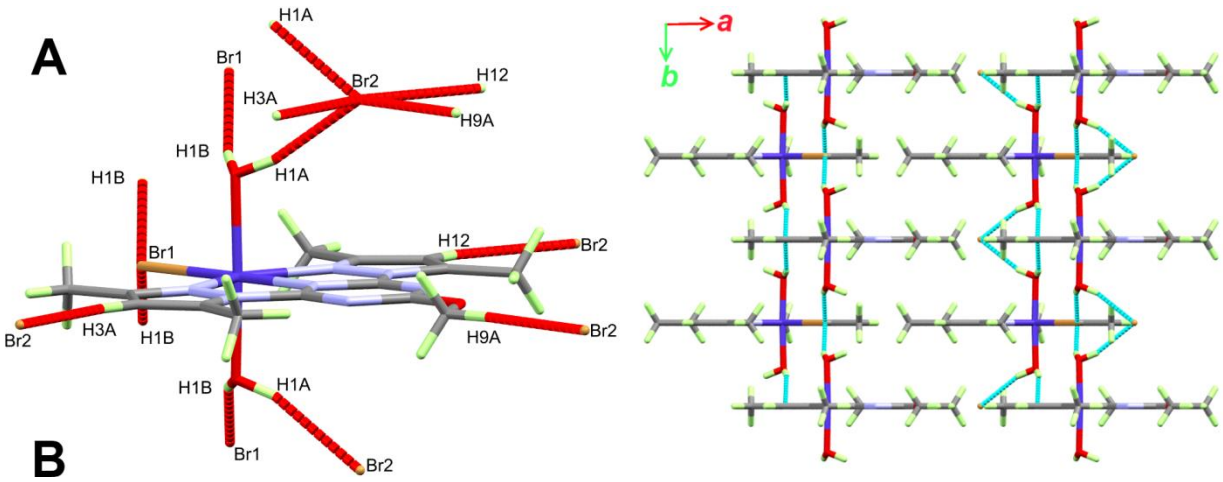

Figure 3. Important contacts (**A**) and packing scheme (**B**) of the $[Co(L)(H_2O)_2Br]Br$ complex via O–H…Br hydrogen bonds along the *ab* plane. All weak C–H…Br interactions were omitted from the packing scheme for better clarity.

Table 3. Hydrogen bond parameters in the $[Co(L)(H_2O)_2Br]Br$ complex.

Atoms	D-H (Å)	H…A (Å)	D…A (Å)	D-H…A (°)	Symm. Code
O1–H1A...Br2	0.86	2.42	3.241(3)	159	
O1–H1B...Br1	0.86	2.49	3.313(3)	162	1 − x,−1/2 + y,1 − z
C3–H3A...Br2	0.93	2.86	3.768(7)	167	1 − x,1/2 + y,−z
C9–H9A...Br2	0.96	2.77	3.709(10)	165	2 − x,1/2 + y,−z
C12–H12...Br2	0.93	2.92	3.809(7)	160	2 − x,1/2 + y,1 − z

3.2. Hirshfeld Analysis

Decomposition of the different intermolecular contacts with the aid of Hirshfeld analysis is important to further inspect the molecular packing at both qualitative and quantitative levels. Using the Crystal Explorer 17.5 program [38], the contacts involved in the molecular packing and their percentages are presented in Figure 4. It is clear that the most dominant contacts are H…H (48.8%), Br…H (17.6%), H…C (11.2%) and O…H (10.1%). The majority of these contacts (except the Br…H) is generally weak and appeared as blue or white regions in the d_{norm} map (Figure S3; Supplementary data). The blue and white colored area represent contacts with longer distance than the vdWs radii sum of the interacting atoms [39–43].

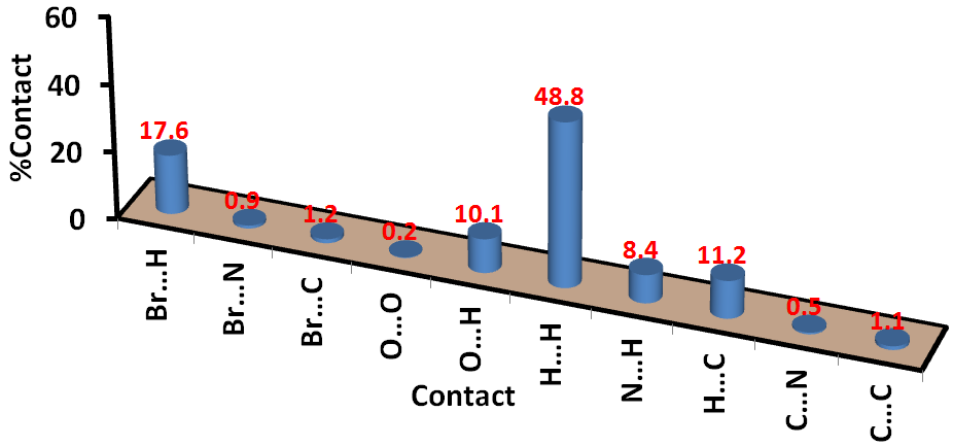

Figure 4. Percentages of all intermolecular contacts in the $[Co(L)(H_2O)_2Br]Br$ complex.

On the other hand, the Br…H contacts appeared as red regions, indicating a shorter distance than the vdWs sum of the Br and H atoms (Figure 5). Additionally, the Br…H contacts appeared as sharp spikes in the fingerprint plot revealed short distance atom-atom interactions. The Br2…H1A (2.307 Å), Br1…H1B (2.368 Å), Br2…H13 (2.655Å), Br2…H9A (2.708 Å), and Br2…H12 (2.781 Å) contacts are the most important.

3.3. Cytotoxic Activity

The free ligand **L** and the four Co (II) complexes were examined for their cytotoxic activities against lung (A-549) and breast (MCF-7) cancer cell lines. The detailed cytotoxicity results using cell viability assay for the studied compounds against these cell lines are given in Tables S1–S10 (Supplementary data). In addition, the effect of concentration of the studied compounds on the cell viability of A-549 cell line is presented graphically in Figure 6. Evaluation of the cytotoxic activity of the studied compounds was performed by detecting the IC_{50} value, which is the concentration required to cause toxic effects in 50% of intact cells. The cytotoxicity activity of the free **L** against the lung A-549 cell line is 1245.37 ± 45.57 µM. For complexes **1**–**4**, the IC_{50} values were determined to be 367.60 ± 14.74, 486.25 ± 20.27, 694.35 ± 25.87, and 353.13 ± 13.04 µM, respectively. The order of the cytotoxic activity is **4** > **1** > **2** > **3** > **L**. As a result, the nitrato complex **4** has the

best cytotoxic activity against lung carcinoma. Additionally, the bromo complex (**1**) has better cytotoxic activity than the chloro compound (**2**).

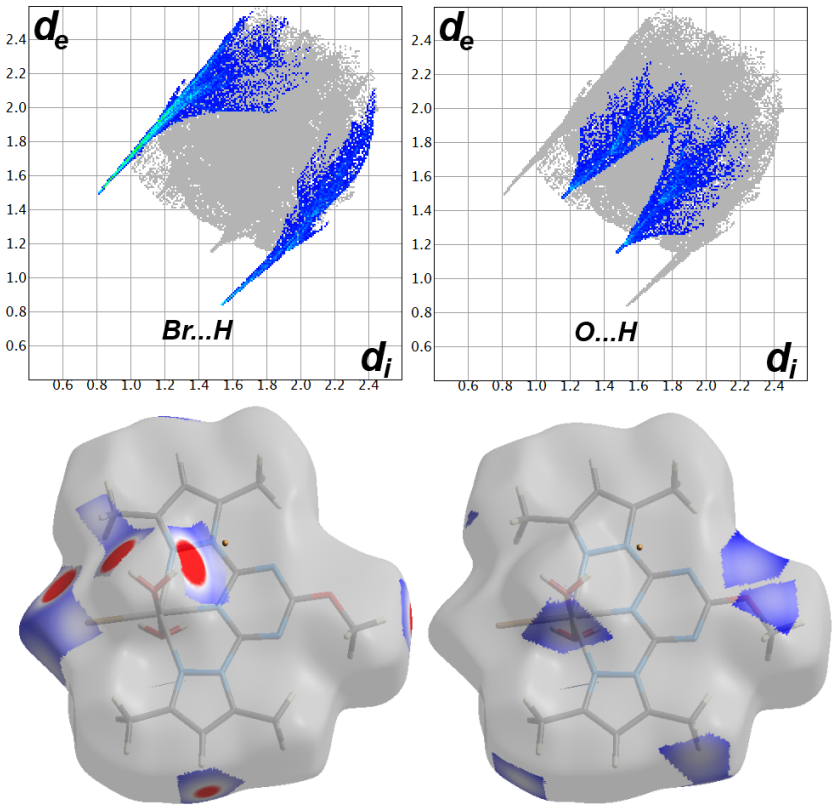

Figure 5. The decomposed d_{norm} and fingerprint plots of the Br…H and O…H interactions in the $[Co(L)(H_2O)_2Br]Br$ complex.

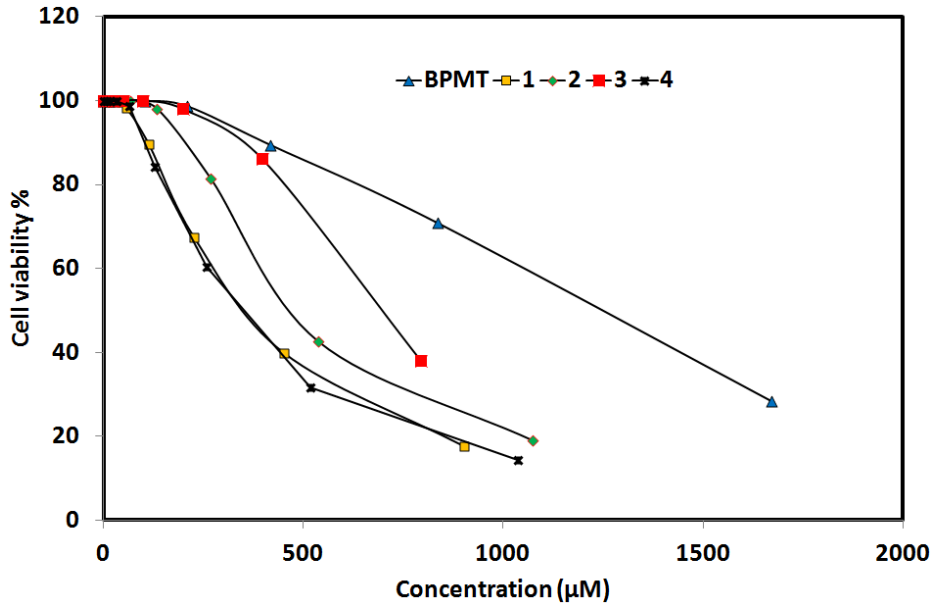

Figure 6. The cytotoxic activity of the studied compounds against A-549 cell line.

On the other hand, the effect of concentration of the studied compounds on the cell viability of MCF-7 cell line is presented graphically in Figure 7. The order of the cytotoxic activity of the studied compounds was found to be **4** > **2** > **1** > **3** > **L**. The IC_{50} values of the studied complexes indicated that complex **4** (IC_{50} = 431.23 ± 20.28 µM) slightly

outperformed complexes **1** (439.27 ± 19.76 μM) and **2** (IC_{50} = 438.79 ± 19.17 μM) against the MCF-7 cell line. The IC_{50} value is the least for complex **3** (674.40 ± 30.85 μM) and the free L ligand (940.77 ± 54.22 μM). In both cell lines, the perchlorate complex has the worst cytotoxic activity. Notably, all the studied complexes comprised the [Co (L)] unit but differed in the structure of the small coordinating groups and the anion as well. These differences could have a significant impact on the cytotoxic activity of the studied complexes. For *cis*platin as a positive control and in the same experimental conditions, the IC_{50} values against the A-549 and MCF-7 cell lines were determined to be 25.01 ± 2.29 and 15.31 ± 1.76 μM, respectively. Hence, the cytotoxic activity of the studied Co (II) complexes was considered weak against both cell lines. Notably, the free salts $CoCl_2$ and $Co(NO_3)_2.6H_2O$ have no or very weak cytotoxic activities against both cell lines (Tables S11–S14, Supplementary data).

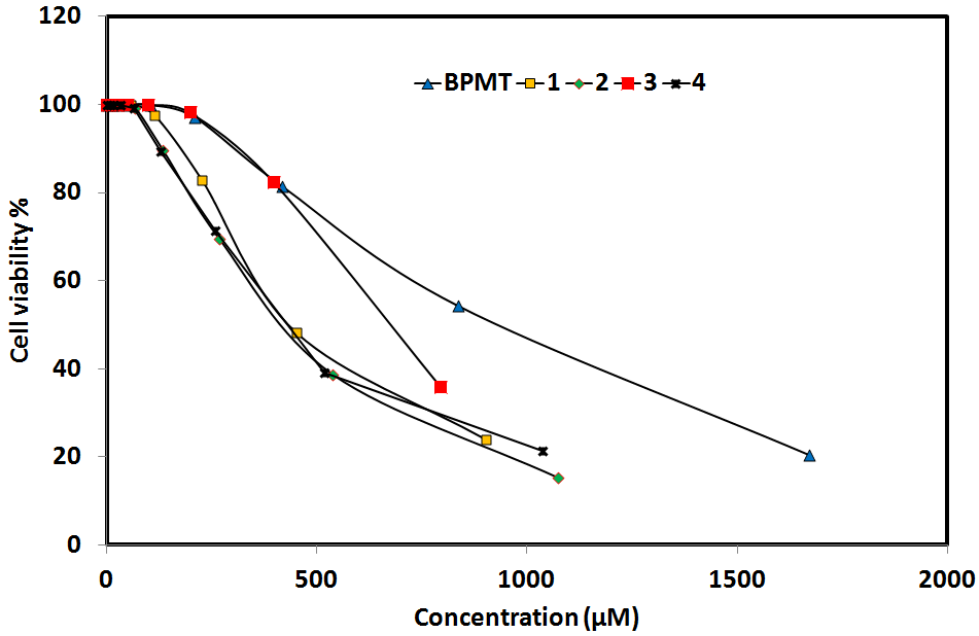

Figure 7. The cytotoxic activity of the studied compounds against MCF-7 cell line.

4. Conclusions

The X-ray single-crystal structure of the new $[Co(L)(H_2O)_2Br]Br$ complex was determined and its molecular and supramolecular structural aspects have been discussed. It comprised a hexa-coordinated Co (II) ion with one **L** ligand as a tridentate pincer chelate, two trans water molecules at the axial positions, and one equatorial bromide ion. The cationic $[Co(L)(H_2O)_2Br]^+$ inner sphere was neutralized by one free uncoordinated bromide ion in the outer sphere. Its supramolecular structure was controlled by H…H (48.8%), Br…H (17.6%), H…C (11.2%), and O…H (10.1%) intermolecular interactions, where the Br…H contacts are the most important. Additionally, the cytotoxic activity of four structurally related Co (II) complexes of the pincer ligand **L** was evaluated against lung (A-549) and breast (MCF-7) cell lines. The results indicated the variation in the cytotoxic activity of the studied Co (II) complexes depending on the small coordinating group and the nature of the anion. Complex **4** had the best activity against breast cancer (MCF-7) and lung (A-549) cancer cell lines, where its cytotoxic activity was two and three times better than the free ligand (**L**), respectively.

Supplementary Materials: The following supporting information can be downloaded at: https://www.mdpi.com/article/10.3390/cryst12050741/s1. Physicochemical characterizations; crystal structure determination; synthesis of L; synthesis of complexes 2–4; Method S1. Evaluation of cytotoxic effects; Figure S1. 1H and 13C NMR spectra of the ligand (L); Figure S2. FTIR spectra of

complex 1; Figure S3. Hirshfeld maps for the [Co(L)(H2O)2Br]Br complex; Table S1. Evaluation of the cytotoxicity of 1 against the A-549 cell line. Table S2. Evaluation of the cytotoxicity of 2 against the A-549 cell line; Table S3. Evaluation of the cytotoxicity of 3 against the A-549 cell line; Table S4. Evaluation of the cytotoxicity of 4 against the A-549 cell line; Table S5. Evaluation of the cytotoxicity of L against the A-549 cell line. Table S6; Evaluation of the cytotoxicity of 1 against the MCF-7 cell line; Table S7. Evaluation of the cytotoxicity of 2 against the MCF-7 cell line; Table S8. Evaluation of the cytotoxicity of 3 against the MCF-7 cell line; Table S9. Evaluation of the cytotoxicity of 4 against the MCF-7 cell line; Table S10. Evaluation of the cytotoxicity of L against the MCF-7 cell line; Table S11. Evaluation of the cytotoxicity of CoCl2 against the A-549 cell line; Table S12. Evaluation of the cytotoxicity of Co(NO3)2.6H2O against the A-549 cell line; Table S13. Evaluation of the cytotoxicity of CoCl2 against the MCF-7 cell line; Table S14. Evaluation of the cytotoxicity of Co(NO3)2.6H2O against the MCF-7 cell line. Examples can be found at http://www.mdpi.com/2076-2615/6/6/40/htm (accessed on 13 May 2022). References [44,45] are cited in the supplementary materials.

Author Contributions: Conceptualization, H.M.R., A.E.-F. and S.M.S.; methodology, H.M.R. and S.M.S.; software, S.M.S. and N.D.; formal analysis, H.M.R., A.A.M.A., N.D., A.E.-F. and S.M.S.; investigation, A.A.M.A. and H.M.R.; resources, H.M.R., A.E.-F., N.D., A.A.M.A. and S.M.S.; writing—original draft preparation, H.M.R., A.E.-F., N.D., A.A.M.A. and S.M.S.; writing—review and editing, H.M.R., A.E.-F., N.D. and S.M.S.; supervision, H.M.R., A.E.-F. and S.M.S. All authors have read and agreed to the published version of the manuscript.

Funding: This research received no external funding.

Institutional Review Board Statement: Not applicable.

Informed Consent Statement: Not applicable.

Data Availability Statement: Not applicable.

Acknowledgments: The authors acknowledge the Scientific and Technological Research Application and Research Center, Sinop University, Turkey, for the use of the Bruker D8 QUEST diffractometer.

Conflicts of Interest: The authors declare no conflict of interest.

References

1. Silen, J.L.; Lu, A.T.; Solas, D.W.; Gore, M.A.; MacLean, D.; Shah, N.H.; Coffin, J.M.; Bhinderwala, N.S.; Wang, Y.; Tsutsui, K.T.; et al. Screening for novel antimicrobials from encoded combinatorial libraries by using a two-dimensional agar format. *Antimicrob. Agents Chemother.* **1998**, *42*, 1447–1453. [CrossRef] [PubMed]
2. Zhou, C.; Min, J.; Liu, Z.; Young, A.; Deshazer, H.; Gao, T.; Chang, Y.T.; Kallenbach, N.R. Synthesis and biological evaluation of novel 1,3,5-triazine derivatives as antimicrobial agents. *Bioorg. Med. Chem. Lett.* **2008**, *4*, 1308–1311. [CrossRef] [PubMed]
3. Koc, Z.E.; Bingol, H.; Saf, A.O.; Torlak, C.A. Synthesis of novel tripodal-benzimidazole from 2,4,6-tris(p-formylphenoxy)-1,3,5-triazine: Structural, electrochemical and antimicrobial studies. *J. Hazard. Mater.* **2010**, *183*, 251–255. [CrossRef] [PubMed]
4. Desai, N.; Makwana, A.H.; Rajpara, K. Synthesis and study of 1,3,5-triazine based thiazole derivatives as antimicrobial agents. *J. Saudi Chem. Soc.* **2016**, *20*, S334–S341. [CrossRef]
5. Vembu, S.; Pazhamalai, S.; Gopalakrishnan, M. Potential antibacterial activity of triazine dendrimer: Synthesis and controllable drug release properties. *Bioorg. Med. Chem.* **2015**, *23*, 4561–4566. [CrossRef]
6. Foster, B.J.; Harding, B.J.; Leyland-Jones, B.; Hoth, D. Hexamethylmelamine: A critical review of an active drug. *Cancer Treat. Rev.* **1986**, *13*, 197–217. [CrossRef]
7. Ono, M.; Kawahara, N.; Goto, D.; Wakabayashi, Y.; Ushiro, S.; Yoshida, S.; Izumi, H.; Kuwano, M.; Sato, Y. Inhibition of tumor growth and neovascularization by an antigastric ulcer agent, irsogladine. *Cancer Res.* **1996**, *56*, 1512–1516.
8. Tranchand, B.; Catimel, G.; Lucas, C.; Sarkany, M.; Bastian, G.; Evene, E.; Guastalla, J.P.; Négrier, S.; Rebattu, P.; Dumortier, A.; et al. Phase I clinical and pharmacokinetic study of S9788, a new multidrug-resistance reversal agent given alone and in combination with doxorubicin to patients with advanced solid tumors. *Cancer Chemother. Pharmacol.* **1998**, *41*, 281–291. [CrossRef]
9. Maeda, M.; Ligo, M.; Tsuda, H.; Fujita, H.; Yonemura, Y.; Nakagawa, K.; Endo, Y.; Sasaki, D. Antimetastatic and antitumor effects of 2,4-diamino-6-(pyridine-4-yl)-1,3,5-triazine (4PyDAT) on the high lung metastatic colon 26 tumor in mice. *Anticancer Drug Des.* **2000**, *15*, 217–222.
10. Kumar, P.V.; Tusi, S.; Tusi, Z.; Joshi, M.; Bajpai, S. Synthesis and biological activity of substituted 2,4,6-*s*-triazines. *Acta Pharm.* **2004**, *54*, 1–12.
11. Al-Zaydi, K.M.; Khalil, H.H.; El-Faham, A.; Khattab, S.N. Synthesis, characterization and evaluation of 1,3,5-triazine aminobenzoic acid derivatives for their antimicrobial activity. *Chem. Cent. J.* **2017**, *11*, 39. [CrossRef] [PubMed]

12. Soliman, S.M.; Massoud, R.A.; Al-Rasheed, H.H.; El-Faham, A. Syntheses and Structural Investigations of Penta-Coordinated Co(II) Complexes with Bis-Pyrazolo-*s*-Triazine Pincer Ligands, and Evaluation of Their Antimicrobial and Antioxidant Activities. *Molecules* **2021**, *26*, 3633. [CrossRef] [PubMed]
13. Aksenov, A.V.; Aksenova, I.V. Use of the ring opening reactions of 1,3,5-triazines in organic synthesis. *Chem. Heterocycl. Comp.* **2009**, *45*, 130–150. [CrossRef]
14. Sessler, J.L.; Doctrow, S.R.; McMurry, T.J.; Lippard, S.J. (Eds.) *Medicinal Inorganic Chemistry*; American Chemical Society: Washington, DC, USA, 2003.
15. Hemaida, H.A.E.; Dissouky, A.A.E.; Sadek, S.M.M. Potential antifouling agents: Copper, cobalt, and nickel complexes of 3-(2-acetyl pyridylidene) hydrazino-5,6- diphenyl-1,2,4-triazine. *Egypt. J. Aquat. Res.* **2005**, *31*, 45–56.
16. Katugampala, S.; Perera, I.C.; Nanayakkara, C.; Perera, T. Synthesis, Characterization, and Antimicrobial Activity of Novel Sulfonated Copper-Triazine Complexes. *Bioinorg. Chem. Appl.* **2018**, *2018*, 2530851. [CrossRef]
17. Al-Hazmi, G.A.; Abou-Melha, K.S.; Althagafi, I.; El-Metwaly, N.; Shaaban, F. Synthesis and structural characterization of oxovanadium(IV) complexes of dimedone derivatives. *Appl. Organomet. Chem.* **2020**, *34*, e5672. [CrossRef]
18. El-Gammal, O.A.; Mohamed, F.S.; Rezk, G.N.; El-Bindary, A.A. Synthesis, Characterization, Catalytic, DNA Binding and Antibacterial Activities of Co(II), Ni(II) and Cu(II) Complexes with New Schiff Base Ligand. *J. Mol. Liq.* **2021**, *326*, 115223. [CrossRef]
19. Sakurai, H.; Kojima, Y.; Yoshikawa, Y.; Kawabe, K.; Yasui, H. Antidiabetic Vanadium(IV) and Zinc(II) Complexes. *Coord. Chem. Rev.* **2002**, *226*, 187–198. [CrossRef]
20. Vivekanand, B.; Mahendra, R.K.; Mruthyunjayaswamy, B.H.M. Synthesis, Characterization, Antimicrobial, DNA-Cleavage and Antioxidant Activities of 3-((5-Chloro-2-Phenyl-1H-Indol-3-Ylimino)Methyl)Quinoline-2(1H)-Thione and Its Metal Complexes. *J. Mol. Struct.* **2015**, *1079*, 214–224. [CrossRef]
21. Ghaib, A.; Ménager, S.; Vérité, P.; Lafont, O. Synthesis of variously 9,9-dialkylated octahydropyrimido [3,4-a]-s-triazines with potential antifungal activity. *IL Farm.* **2002**, *57*, 109–116. [CrossRef]
22. Lübbers, T.; Angehrn, P.; Gmünder, H.; Herzig, S.; Kulhanek, J. Design, synthesis, and structure-activity relationship studies of ATP analogues as DNA gyrase inhibitors. *Bioorg. Med. Chem. Lett.* **2000**, *10*, 821–826. [CrossRef]
23. Soliman, S.M.; El-Faham, A. One pot synthesis of two Mn(II) perchlorate complexes with *s*-triazine *NNN*-pincer ligand; molecular structure, Hirshfeld analysis and DFT studies. *J. Mol. Struct.* **2018**, *1164*, 344–353. [CrossRef]
24. Soliman, S.M.; El-Faham, A. Synthesis, Molecular and Supramolecular Structures of New Mn(II) Pincer-Type Complexes with *s*-Triazine Core Ligand. *J. Coord. Chem.* **2018**, *71*, 2373–2388. [CrossRef]
25. Soliman, S.M.; Almarhoon, Z.; Sholkamy, E.N.; El-Faham, A. *Bis*-pyrazolyl-*s*-triazine Ni(II) pincer complexes as selective gram positive antibacterial agents; synthesis, structural and antimicrobial studies. *J. Mol. Struct.* **2019**, *1195*, 315–322. [CrossRef]
26. Soliman, S.M.; Elsilk, S.E.; El-Faham, A. Synthesis, structure and biological activity of zinc(II) pincer complexes with 2,4-*bis*(3,5-dimethyl-1*H*-pyrazol-1-yl)-6-methoxy-1,3,5-triazine. *Inorg. Chim. Acta* **2020**, *508*, 119627. [CrossRef]
27. Soliman, S.M.; El-Faham, A.; Elsilk, S.E. Novel 1D polymeric Cu(II) complexes via Cu(II)-assisted hydrolysis of 2,4-bis(3,5-dimethyl-1H-pyrazol-1-yl)-6-methoxy-1,3,5-triazine pincer ligand; Synthesis, structure, and antimicrobial activities. *Appl. Organomet. Chem.* **2020**, *34*, e5941. [CrossRef]
28. Abumelha, H.M.; Alkhatib, F.; Alzahrani, S.; Abualnaja, M.; Alsaigh, S.; Alfaifi, M.Y.; Althagafi, I.; El-Metwaly, N. Synthesis and Characterization for Pharmaceutical Models from Co(II), Ni(II) and Cu(II)-Thiophene Complexes; Apoptosis, Various Theoretical Studies and Pharmacophore Modeling. *J. Mol. Liq.* **2021**, *328*, 115483. [CrossRef]
29. Abou-Melha, K.S.; Al-Hazmi, G.A.; Althagafi, I.; Alharbi, A.; Shaaban, F.; El-Metwaly, N.M.; El Bindary, A.A.; El-Bindary, M.A. Synthesis, Characterization, DFT Calculation, DNA Binding and Antimicrobial Activities of Metal Complexes of Dimedone Arylhydrazone. *J. Mol. Liq.* **2021**, *334*, 116498. [CrossRef]
30. Li, Y.; Li, Y.; Liu, X.; Yang, Y.; Lin, D.; Gao, Q. The Synthesis, Characterization, DNA/Protein Interaction, Molecular Docking and Catecholase Activity of Two Co(II) Complexes Constructed from the Aroylhydrazone Ligand. *J. Mol. Struct.* **2020**, *1202*, 127229. [CrossRef]
31. Lara, B.-S.; Ruiz, G.-C.; Sosa, B.-L.R.; Mora, G.-I.; Álamo, F.-M.; Behrens, B.-N. Cytotoxic Copper(II), Cobalt(II), Zinc(II), and Nickel(II) Coordination Compounds of Clotrimazole. *J. Inorg. Biochem.* **2012**, *114*, 82–93. [CrossRef]
32. Soliman, S.M.; Elsilk, S.E.; El-Faham, A. Syntheses, structure, Hirshfeld analysis and antimicrobial activity of four new Co(II) complexes with *s*-triazine-based pincer ligand. *Inorg. Chim. Acta* **2020**, *510*, 119753. [CrossRef]
33. Sheldrick, G.M. SHELXT—Integrated space-group and crystal-structure determination. *Acta Cryst. A* **2015**, *71*, 3–8. [CrossRef] [PubMed]
34. Sheldrick, G.M. Crystal structure refinement with SHELXL. *Acta Cryst. C* **2015**, *71*, 3–8. [CrossRef]
35. Farrugia, L.J. WinGX and ORTEP for Windows: An update. *J. Appl. Crystallogr.* **2012**, *45*, 849–854. [CrossRef]
36. Bruker. *APEX2, SAINT, SADABS, and XSHELL*; Bruker AXS Inc.: Madison, WI, USA, 2013.
37. Macrae, C.F.; Sovago, I.; Cottrell, S.J.; Galek, P.T.A.; McCabe, P.; Pidcock, E.; Platings, M.; Shields, G.P.; Stevens, J.S.; Towler, M.; et al. Mercury 4.0: From visualization to analysis, design and prediction. *J. Appl. Cryst.* **2020**, *53*, 226–235. [CrossRef]
38. Turner, M.J.; McKinnon, J.J.; Wolff, S.K.; Grimwood, D.J.; Spackman, P.R.; Jayatilaka, D.; Spackman, M.A. *Crystal Explorer 17*; University of Western Australia: Perth, Australia, 2017; Available online: http://hirshfeldsurface.net (accessed on 1 July 2021).
39. Hirshfeld, F.L. Bonded-atom fragments for describing molecular charge densities. *Theor. Chim. Acta* **1977**, *44*, 129–138. [CrossRef]

40. Spackman, M.A.; Jayatilaka, D. Hirshfeld surface analysis. *Cryst. Eng. Comm.* **2009**, *11*, 19–32. [CrossRef]
41. Spackman, M.A.; McKinnon, J.J. Fingerprinting intermolecular interactions in molecular crystals. *Cryst. Eng. Commun.* **2002**, *4*, 378–392. [CrossRef]
42. Bernstein, J.; Davis, R.E.; Shimoni, L.; Chang, N.L. Patterns in Hydrogen Bonding: Functionality and Graph Set Analysis in Crystals. *Angew. Chem. Int. Ed.* **1995**, *34*, 1555–1573. [CrossRef]
43. McKinnon, J.J.; Jayatilaka, D.; Spackman, M. Towards quantitative analysis of intermolecular interactions with Hirshfeld surfaces. *Chem. Commun.* **2007**, *37*, 3814–3816. [CrossRef]
44. Mosmann, T. Rapid colorimetric assay for cellular growth and survival: Application to proliferation and cytotoxicity assays. *J. Immunol. Methods* **1983**, *65*, 55–63. [CrossRef]
45. Gomha, S.M.; Riyadh, S.M.; Mahmmoud, E.A.; Elaasser, M.M. Synthesis and Anticancer Activities of Thiazoles, 1,3-Thiazines, and Thiazolidine Using Chitosan-Grafted-Poly(vinylpyridine) as Basic Catalyst. *Heterocycles* **2015**, *91*, 1227–1243.